

## Modelling of thermoradiative-convective drying process of products of plant origin

Igor Dubkovetsky, Nataliya Melnyk,  
Tetiana Burlaka, Yulia Tkachuk

National University of Food Technologies, Kyiv, Ukraine

---

### Abstract

---

#### Keywords:

Drying  
Mushrooms  
Hawthorn  
Apple  
Thermoradiation  
Convection

**Introduction.** The aim of the research was to develop the basics of simulating processes of the simultaneous influence of thermoradiation and convection during drying of plant raw materials.

**Materials and methods.** Cultivated mushrooms, hawthorn, winter varieties of apples and apple snacks were used in the study. Drying was carried out in pulsed heating-cooling mode, while heating was carried out by a heat pump and infrared rays to a set temperature with a wavelength in the range of 1.2–4  $\mu\text{m}$  with a flux density of 8  $\text{kW/m}^2$ .

**Results and discussion.** Modelling of thermoradiative-convective drying of cultivated mushrooms was carried out when the moisture content decreased from 809 to 30% within 80 min, and for hawthorn, the moisture content decreased from 330 to 38% in 60 min. The drying time for apples was 60 min, and the drying time for apple snacks was 70 min, since snacks contain sugar, which has the property of retaining moisture.

According to the developed mathematical model of the drying process, the diffusion capacity of moisture was calculated for all studied products. It was the highest for cultivated mushrooms,  $9.5810^{-4} \text{ m}^2/\text{s}$ , due to the lowest density of  $750 \text{ kg/m}^3$  and the highest porosity, which led to deeper penetration of infrared radiation with a thermal diffusion coefficient of  $1.011 \times 10^{-3} \text{ 1/K}$ . The density of hawthorn was  $1173.4 \text{ kg/m}^3$ , the moisture diffusion coefficient was  $6.8 \times 10^{-7} \text{ m}^2/\text{s}$  and a thermal diffusion coefficient was  $0.51 \times 10^{-2} \text{ 1/K}$  because the hawthorn fruits were spherical and were placed in the dryer as a heap. Apples and apple snacks were cut into slices 4–6 mm thick. The density of apples was  $880 \text{ kg/m}^3$ , the moisture diffusion coefficient was  $8.48 \times 10^{-5} \text{ m}^2/\text{s}$ , and the thermal diffusion coefficient was  $3.096 \times 10^{-5} \text{ 1/K}$ . Apple snacks were made by blanching apple cores in sugar syrup before drying, which led to a decrease in the moisture diffusion coefficient to  $8.28 \times 10^{-6} \text{ m}^2/\text{s}$ , an increase of density to  $965 \text{ kg/m}^3$  and a thermal diffusion coefficient to  $4.06 \times 10^{-2} \text{ 1/K}$  compared to apple slices.

Modelling the interaction of convective and thermoradiative energy supply in pulse mode allows to ensure the maximum technological effect.

**Conclusions.** The mathematical model of thermoradiative-convective drying allows to display in an analytical form the main features of the simultaneous influence of convective and thermoradiative energy supply during drying of high-moisture materials.

---

#### Article history:

Received  
21.02.2023  
Received in  
revised form  
20.12.2023  
Accepted  
29.12.2023

---

#### Corresponding author:

Igor  
Dubkovetsky  
E-mail:  
dubkov78@ukr.net

---

#### DOI:

10.24263/2304-  
974X-2023-12-4-4

## Introduction

The creation of combined dehydration technologies in one dryer allows to make a detailed analysis and combine the advantages of different energy supply methods and minimize the disadvantages of each individual drying method.

The method of combined drying and the development of new drying units with combined modes, which will ensure a significant increase in the intensity of the process, saving electricity and improving the quality of products, are considered a promising and economically feasible direction for obtaining dehydrated products. Solving the problem of resource conservation is also complicated by the fact that high-moisture materials are characterized by high hydrophilicity and significant variability of thermophysical, optical, physical-mechanical and structural properties, which cannot be described mathematically in one model. Sabarez (2015) described the modelling of transport mechanisms involved in the process of drying of food products and obtained models for the industrial drying process. It is engaged in modelling the characteristics of drying hawthorn fruits in microwave-convective conditions, created a laboratory microwave convection dryer and obtained an effective moisture permeability ranging from  $9.29 \times 10^{-10}$  to  $8.81 \times 10^{-9}$  m<sup>2</sup>/s. Argyropoulos et al. (2011) evaluated convection, hot air in combination with microwave vacuum and freeze-drying of mushrooms and found that the thickness of the material is decisive in drying when dehydrating the microwave vacuum to 6% moisture for 25–30 min, and Maisnam et al. (2017) described recent advances in traditional drying of food. Arumuganathan et al. (2011) obtained a mathematical model of drying kinetics of mushrooms in a fluidized bed dryer, described the model of Wang and Singh and established the best drying behaviour of mushroom slices. It was shown that a thin-layer model of convective and microwave-convective drying and proposed drying equipment for it (Bhattacharya et al., 2015). At the convectively drying of cherry tomatoes at a temperature of 60 °C, taking into account their shrinkage, the diffusion coefficients for unpeeled tomatoes to be  $9.16 \times 10^{-12}$  m<sup>2</sup>/s, and for peeled tomatoes to be  $1.53 \times 10^{-10}$  m<sup>2</sup>/s (Bennamoun et al. 2015). Gunhan et al. (2004) determined the quality parameters of bay leaf drying, and Menges et al. (2006) mathematically modelled thin-layer drying of apples. According to the obtained model, it is possible to predict the effect of product moisture, temperature, and air speed in the chamber with the help of a constant model.

Zecchi et al. (2011) compared by modelling and minimizing the duration of combined convective-vacuum drying of mushrooms and parsley, and developed a set of simple diffusion models for vacuum-convective drying, and Sharma et al. (2005) develop mathematical models of thin-layer drying of onion particles by infrared radiation and determined the rational radiation power of 300–500 W at an air speed of 1.0 m/s and an air temperature of 35 °C.

During infrared microwave drying of a peach it was found that increasing the drying power in the microwave oven and the power of infrared radiation leads to an increase in the rate of peach dehydration and a decrease in energy consumption (Wang et al., 2006). Coşkun (2017) applied ten-layer drying models for tomato slices dried with a closed-cycle heat pump, found that the moisture diffusivity ranged from  $8.28 \times 10^{-11}$  to  $1.41 \times 10^{-10}$  m<sup>2</sup>/s.

The combining thermoradiative and convective dehydration in hybrid (mixed) drying technologies is not sufficiently studied. This technologies achieve a synergistic effect, which leads to a reduction in duration and energy consumption. Previous studies of drying of products of plant origin showed that combined drying was industrially important (Dubkovetskiy et al., 2019). The products were heated by infrared rays and the surrounding air in the dryer was heated by a heat pump condenser. Thermoradiative drying was an

effective method of dehydration. The energy of radiation-infrared emitters was transferred to the surface of the product without heating the surrounding air. The radiation reached the surface of the material, penetrated it, and then turned into heat. During the drying process, the absorbing, reflecting and transmissive properties of the radiation of the dried material were constantly changing due to the decrease in the water content in it. Infrared radiation has advantages: high heat transfer coefficients, short drying time and easy control of the temperature of the material. For the scientific substantiation of technological regimes it was necessary to understand clearly and represent the physical essence of the mechanisms of phenomena occurring in the dryer, to analyse their interconnection and the degree of mutual influence. Taking into account the specificity of the object of biological nature (suspension containing a living cell culture) it was necessary to find the restrictions imposed in this case. Since all parameters were internally interconnected, the development of a new drying technology was a multi-parameter task, the solution of which was possible using mathematical modelling methods.

The aim of this research was to develop the basics of simulating processes of the simultaneous influence of thermoradiation and convection during drying of plant raw materials, as well as the development of a thermoradiative-convective drying unit.

## **Materials and methods**

### **Materials**

Cultivated mushrooms, hawthorn, winter varieties of apples, and apple snacks were subjects of the present research.

### **Thermoradiative-convective drying unit with a heat pump**

Process of food drying was conducted using a thermoradiative-convective device with a heat pump (Figure 2). Inside the drying chamber, on the side walls, nodes of infrared radiation emitters were fixed, consisting of infrared radiation emitters 2, which can be moved relative to reflectors 3. Reflector 3 can rotate around the infrared radiation emitter, which made it possible to change the amount of sample irradiation and the product coverage area 16 dryers on trays. Four-side irradiation of the product in the center of the tray from emitters fixed on different side walls of the dryer, and irradiating the tray from below and above, made it possible to compensate for the loss of radiation intensity in the farthest corners of the reflector due to overlapping rays. The design of the radiator unit included two couples of radiation-infrared radiators and reflectors directed in different directions and irradiating the tray from the top and the bottom. The design of the device of infrared radiation emitters allowed the use of both "light" and "dark" infrared radiation emitters for drying products.

A combined thermoradiative-convective method of drying food products was provided in the device. Convective heating of the air was provided in the condenser 25 of the heat pump, and thermoradiative heating – by radiation-infrared emitters 2. The complex interaction of convective and thermoradiative energy supply in pulse mode allowed to ensure the maximum technological effect and achieve the technical result of the invention.



Mushrooms



Hawthorn



Apples



Apple snacks

**Figure 1. Appearance of dry products**

Air was supplied in the chamber under the lower shelves, air pressure losses took place when moving from the lower to the upper shelves due to pneumatic resistance. To reduce stagnant zones and evenly distribute air, technological channels 15 for additional air supply, as well as channels 12 for air removal, located in the side walls of the dryer, were designed. Channels made it possible to ensure flow turbulence at low speeds, where in addition to longitudinal movement (from bottom to top), transverse movement also occurred. The formation of turbulent flows over the surface of the dried semi-finished product made it possible to remove moisture from the boundary layer intensively. Supplying heat from the condenser 25 to the product and removing moisture produced by the action of infrared emitters 2 occurred by air.

### **Experimental devices**

To save energy resources, the exhaust air reached the circulation pipe 14 (Figure 2), and then it entered the air distribution mechanism 18, which was designed in the form of a gate valve with a partial overlap of the cross section of the pipes. In the distribution mechanism, part of the exhaust air was sucked in by the centrifugal fan 20 and cooled the condenser of the heat pump 25, and the other part is sucked into the evaporator 19 of the heat pump by the

axial fan 21. When the damper 18 was completely closed, the centrifugal fan 20 sucked in all air from the environment and cooled the condenser 25, and all the exhaust air from the circulation pipe 14 was sent to the evaporator 19 of the heat pump. When the shutter 18 was fully opened, all the exhaust air reached the condenser 25 of the heat pump, due to which a softened and humidified drying mode was provided, and the evaporator 19 of the heat pump used exhaust heat from the environment (air, earth, water). The greatest technological effect was achieved when the shutter was covered for 20–80%

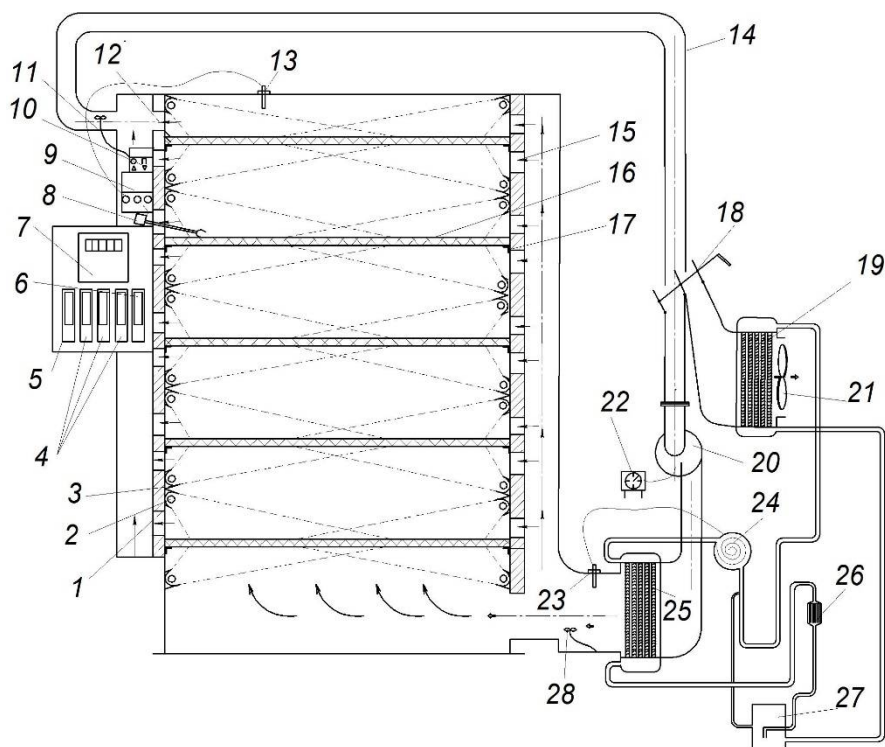


**Figure 2. Scheme of thermoradiative-convective drying device with heat pump:**

- |  |  |
|--|--|
| 1 – drying chamber;  | 15 – technological channels for air supply;  |
| 2 – infrared radiation emitter;  | 16 – dryer trays;  |
| 3 – reflector;   | 17 – shelves for trays;  |
| 4 – automatic dryer switch;  | 18 – sliding door;   |
| 5 – relay;   | 19 – heat pump evaporator;   |
| 6 – automatic switch;  | 20 – centrifugal fan;  |
| 7 – energy consumption counter;  | 21 – axial fan;  |
| 8 – thermocouples;   | 22 – block of automatic adjustment of the speed of movement of the coolant;        |
| 9 – automatic temperature control unit;  | 23 – contact sensor at the entrance to the drying chamber;                         |
| 10 – regulator of relative moisture of air;                                      | 24 – compressor;   |
| 11 – sensor for measuring relative moisture at the exit from the drying chamber; | 25 – heat pump condenser;  |
| 12 – technological channels for air removal;                                     | 26 – throttle;   |
| 13 – contact sensor at the exit from the drying chamber;                         | 27 – separator;  |
| 14 – circulation pipe;   | 28 – sensor for measuring relative moisture at the entrance to the drying chamber. |

Contact sensors 13 and 23 were placed in the cabinet of the drying chamber, which sent a signal to turn on the thermoradiative generators and the heat pump together or separately according to the set air temperature at the entrance to the dryer in pulse mode "heating – cooling". The sensor 13 sent a signal to the relay 5 and turned on and off the radiation-infrared emitters 2. When the set temperature was reached, the contacts of the thermostat 23 opened and the electric motor of the heat pump compressor stopped. When the heat pump was turned off, the heated refrigerant (Freon) from the compressor 24 stopped being supplied to the condenser 25. As soon as the drying temperature reached the required value, which was fixed by the sensor 13, the infrared emitters 2 were turned off and the product in the dryer began to cool. When the product was cooled to the limit temperature, the infrared emitters 2 automatically turned on and the drying process was repeated in the same way until the material reached the specified moisture content.

### **Research process procedure**

The prepared raw were dried by thermoradiative-convective method. The drying parameters were set experimentally: the temperature of the coolant in the drying chamber was 60 °C, the speed of air movement in the chamber was 5.5 m/s, specific load was 8.8 kg/m<sup>2</sup>. The amount of radiation by thermoradiative generators was 8 kW/m<sup>2</sup>, the wavelength of tubular "dark" thermoradiative generators was in the range of 2.0–4.0 μm. Air heating was carried out from an external heating element of 2.5 kW/m<sup>2</sup>, the distance between thermoradiative heaters and the product was 14 cm.

Steps of the procedure:

1. Warm up the installation for 10–15 minutes. To do this, it was set the temperature on the controller of the control panel 9 (Figure 2), turn on the fans 20 and 21, the compressor of the heat pump 24 and the radioactive-infrared emitters 2 in sequence.
2. It was chopped the material to be dried (mushrooms, hawthorn, apples and apple snacks, etc.) into thin shavings 2–5 mm thick and place them evenly on the trays of the dryer 16.
3. It was opened the shutter 18 to the specified degree of air suction. When passing through the distribution mechanism, part of the spent coolant from the circulation pipe 14 is sucked by the centrifugal fan and cools the condenser of the heat pump 25, and the other part is sucked into the evaporator of the heat pump 19 by the axial fan 21.
4. It was controlled the specified pulse switching mode of the heat pump capacitor 25 and infrared radiation emitters 2 to ensure rational energy consumption by meter 7.
5. It was controlled control the overheating of the product with the help of installed temperature sensors 8 (thermocouples) immersed in the product, which send a signal to the temperature controller 9 and through the relay turn on the heat capacitor according to the temperature of the product in the pulse mode "heating-cooling" pumps 25 and radioactive-infrared emitters 2.
6. It was controlled the change in the amount of moisture in the heat carrier with the help of installed relative humidity sensors 11, which send signals to the relative humidity regulator 10, and through the relay, the supply to the condenser is switched on and off in pulse mode "heating-cooling" heat pump heated refrigerant and infrared emitters.
7. It was sequentially turned off the power supply of the heat pump compressor 24 and radioactive infrared emitters 2, and after 10 minutes the fans 20 and 21.
8. Let the product rest for 30 minutes, familiarize yourself with the state of the dried material, and unload it from trays 16 of the dryer into a packaging container.

## Processing of research results

Determination of experimental data was carried out according to the algorithm (Aker F., et al., 2022), where we first determine the current mass of moisture in the material at the beginning and during drying, g:

$$M_m = M_i - M_{d,m}, \quad (1)$$

where  $M_m$  is the mass of moisture in the material at the  $i$ -th time of the experiment, g;

$M_i$  is the mass of the material at the  $i$ -th time of the experiment, g;

$M_{d,m}$  is the mass of dry matter in the material for the entire experiment, g:

$$M_{d,m} = M_0 \cdot X_{d,m} / 100, \quad (2)$$

where  $M_0$  is the initial weight of the material before drying, g;  $X_{d,m}$  is the mass fraction of dry matter.

It was determined the moisture content of the material at the  $i$ -th drying time, %:

$$W = (M_m / M_{d,m}) 100 \quad (3)$$

During the drying process, the change in the temperature of the heat carrier, the density of the products, the specific heat capacity of the dry material, the specific heat of vaporization were recorded, and the coefficients of moisture diffusion, heat transfer, and moisture transfer were calculated and entered in Table 1.

Calculation data were determined by building a physical model and compiling a generalizing equation of the influence of molecular diffusion, thermodiffusion, and internal gas pressure on moisture transfer during the interaction of thermoradiation and convection. The complex system of equations was solved by integral Laplace transformations. A software module for calculating the process of drying high initial moisture content materials with thermoradiative-convective energy supply has been developed. The result of the approximation of experimental and calculated data of drying particles of cultivated mushrooms, hawthorn and apples is shown in Figure 4.

## Results and discussion

In case of the thermoradiative-convective method of drying products of plant origin, the following stages of the process took place in sequence:

- Heating, which was accompanied by partial evaporation of moisture;
- Drying, accompanied by evaporation of moisture from the surface and deepening of the evaporation zone.

### Options for setting thermoradiative-convective drying modes

**1. According to air temperature.** When setting the temperature of the air in the chamber and the range of inclusion and exclusion of radiation-infrared emitters 2, the duration of irradiation of the semi-finished product was controlled by the automatic temperature control unit 9, and the control of the supply of heated refrigerant (Freon) from the compressor 24 to the condenser 25 of the heat pump. Consumption of electrical energy was measured using a counter 7 (per kilogram of evaporated moisture or kilograms of finished products). The sensor with a thermostat 13 controlled the temperature at the outlet of the dryer depending on the properties and characteristics of the product, while the infrared radiation emitters 2 were turned on and off. The temperature at the inlet of the dryer and switching the heat pump on and off was controlled with the help of sensor 23. The heat pump and radiation-infrared emitters can be de-energized together or separately with automatic switches 4.

**2. According to air humidity.** You can set the drying mode according to the relative humidity of the air in the dryer chamber. The change in the relative humidity of the air at the entrance and exit from the drying chamber is recorded by sensors 28 and 11, which sent signals to the regulator of relative moisture 10. By setting the relative moisture range on the regulator 10 and through relay 5 switching on and off supply of the heated refrigerant (freon) occurs in pulse mode "heating – cooling" to the condenser 25 of the heat pump from the compressor 24 and infrared emitters 2 together or separately with different relative moisture of the air.

**3. According to product temperature.** Installed temperature sensors 8 (thermocouples), thanks to immersion in the product, allow you to carry out drying modes according to the temperature of the product, and not the temperature of the coolant, which prevents overheating of the raw material and improves the quality of the final product. Thermocouples send a signal to the temperature regulator 9 and through relay 5 turn on the heat pump capacitor 25 and infrared emitters 2 according to the product temperature in pulse mode "heating – cooling".

The measurement of the temperature of the product in the cross section was carried out by thermocouples 8, which sent a signal to the temperature controller 9. Through the relay 5 they supplied of heated refrigerant (Freon) to the condenser 25 of the heat pump from the compressor 24 according to the temperature of the product in the pulsed "heating – cooling" mode, and infrared emitters 2 (with the help of which the irradiation time of the semi-finished product changed) together or separately with different temperature regimes of the product. The drying process can be carried out according to the temperature of the semi-finished product, which was carried out by setting the automatic temperature control regulator 9 and thermocouples 8. The thermocouples were immersed in the drying products, then the product temperature and the range of turning on and off the infrared radiation emitters 2 and putting heated refrigerant (Freon) into the condenser 25 of the heat pump from compressor 24.

Drying was carried out in pulsed heating-cooling mode, while heating was carried out by a heat pump and infrared rays to a set temperature with a wavelength in the range of 1.2-4  $\mu\text{m}$  with a flux density of 8  $\text{kW}/\text{m}^2$ . After reaching the maximum set temperature of air or product during drying or relative Humidity of air, the heat pump and radiation-infrared emitters were turned off and switched to pulse switching mode. The duration of pulse switching on and pauses were correlated as 1:1, 1:2, 1:3, etc., depending on the type of semi-finished product. The duration of pulse activation and pause were correlated as 1:2 and depended on the semi-finished product and the maximum temperature at the exit from the drying chamber, the temperature of the semi-finished product, the temperature at the entrance to the drying chamber or relative moisture installed by the sensors 13, 8, 23 and 11, respectively.

In order to avoid stagnant zones and uniform distribution of air, technological channels for additional supply and removal of air, located in the side walls of the dryer, were provided. In addition to longitudinal movement (from bottom to top), the channels allowed to provide transverse movement. Placing air channels from bottom and top of the nodes of thermoradiative emitters with the simultaneous supply of air from the bottom to the top led to turbulence of air flows at low velocities. The formation of turbulent flows over the surface of the dried product led to more intense removal of moisture from the boundary layer of the product. At the same time, the drying process was accelerated and energy consumption was reduced.

The interaction of the energy of infrared radiation and an additionally installed heat pump, made it possible to reduce energy costs during using the dryer and the drying process, using alternative sources of heat (air, soil, water). The operation of the heat pump was based



on obtaining heat from an alternative source, increasing its temperature and using this heat in the dryer. The air passing through the condenser of the heat pump was heated, which led to a decrease in the relative moisture of the air supplied to the chamber. At the same time, the driving force of the process increased and, as a result, the drying time decreased.

Since high-moisture materials were crushed to intensify the drying process, the material particles can be represented in the form of a straight parallelepiped with sides  $a$ ,  $b$  and height  $h$ , which were in a ratio close to one to each other (Figure 3).

### Mathematical model of the drying process

The mathematical model of the drying process was formulated on the basis of the generalized law of moisture movement, which took into account the flow of moisture, both in the form of vapour and liquid, caused by the presence of a moisture gradient and a temperature gradient in the wet material.

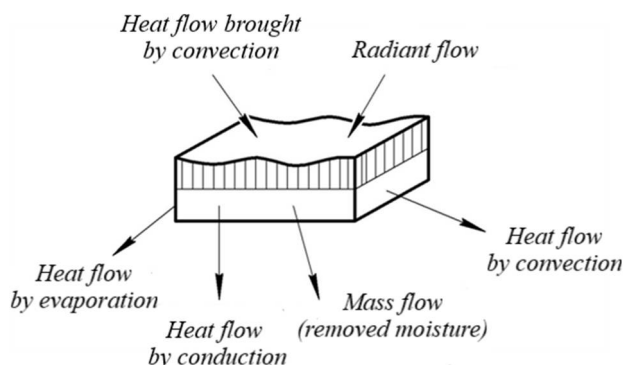


**Figure 3. Model of drying particles of high-moisture materials by the thermoradiative-convective method**

Total moisture flow in the middle of the material (Hayvas 2010):

$$j = -a_m \rho_0 \nabla W - a_m^T \rho_0 \nabla T - a_m^P \rho_0 c_p^a \nabla P \quad (4)$$

where  $\rho_0$  is moisture density,  $\text{kg/m}^3$ ;  $a_m$  is diffusion coefficient,  $\text{m}^2/\text{s}$ ;  $a_m^T$  is thermodiffusion coefficient,  $\text{m}^2/\text{s} \cdot 1/\text{K}$ ;  $a_m^P$  is barodiffusion coefficient,  $\text{m}^2/\text{s} \cdot 1/\text{Pa}$ ;  $\nabla W$  is moisture gradient,  $1/\text{m}$ ;  $\nabla T$  – temperature gradient,  $\text{K}/\text{m}$ ;  $\nabla P$  – pressure gradient,  $\text{Pa}/\text{m}$ .

In this equation, each term describes the contribution to the resulting mass flow of separate physical phenomena: molecular diffusion, thermal diffusion (Sharma et al., 2005), convection mass transfer due to internal gas pressure, and convection moisture transfer (Bennamoun et al., 2015; Pal et al., 1997) caused by a change in the shape and volume of the sample due to deformation caused by shrinkage or swelling. A system of Lykov and Lutsik (Sorokova et al., 2022) equations was obtained that described the dynamics of mass, energy, and momentum transfer processes during the drying process:

$$\frac{\partial T}{\partial \tau} = a_m^T \nabla^2 T + \frac{\varepsilon r}{c} \frac{\partial W}{\partial \tau} - \frac{E_0 (\gamma_T T_0 + \gamma_W W_0)}{c \rho_0} \text{div} \frac{\partial \bar{U}}{\partial \tau}$$

$$\frac{\partial W}{\partial \tau} = a_m \nabla^2 W + a_m^T \nabla^2 T + a_m^P c_p^a \nabla^2 P - \text{div} \frac{\partial \bar{U}}{\partial \tau}; \quad (5)$$

Since the temperature of the coolant in real conditions was less than 80°C (Giri et al., 2007), the phenomena of barodiffusion and thermal moisture conductivity were neglected.

The coefficients of absorption, reflection and transmission of the radiant flow were considered constant. In general, all heat and moisture transfer coefficients, as well as thermodynamic characteristics, depended on the moisture content and temperature. For simplicity, there was assumed that over time  $\tau_k$  coefficients  $a_m, \delta, \lambda, c, r, \varepsilon$  were considered constant. Then, after substitution, the equation was:

$$\begin{cases} \frac{\partial T}{\partial \tau} = a \nabla^2 T + \frac{\varepsilon r}{c} \frac{\partial W}{\partial \tau} \\ \frac{\partial W}{\partial \tau} = a_m \nabla^2 W + a_m^T \nabla T \end{cases} \quad (6)$$

In the heat transfer equation, it was necessary to add a term responsible for infrared heating. Absorption coefficient was denoted as  $A$ . The density of the radiant flow incident on the particle was marked  $q(\tau)$

$$q(\tau) = Aq(\tau) \exp(k(R-r)) \quad (7)$$

where  $r$  is current radius, m;  $q_0$  is density of the heat flow, which was directed to the surface (perceived by surface),  $J/(m^2 \times s)$ ;  $\mu$  is attenuation coefficient,  $\omega$  is reflection coefficient.

Combination of two radiant flows from lamps located on different sides gave heating that did not depend on the  $X$  coordinate.

Thus, the heat transfer equation was:

$$\frac{\partial T}{\partial \tau} = a \nabla^2 T + \frac{\varepsilon r}{c} \frac{\partial W}{\partial \tau} + \frac{Aq}{c \rho_0} \quad (8)$$

Under these conditions, the drying process was described by a system of differential equations in partial derivatives in spherical coordinates, consisting of differential equations of heat and mass transfer for the particle of the product.

$$\begin{cases} \frac{\partial T(r, \tau)}{\partial \tau} = a \left( \frac{d^2 T(r, \tau)}{dr^2} + \frac{2}{r} \frac{dT(r, \tau)}{dr} \right) + \frac{\varepsilon r}{c} \frac{\partial W(r, \tau)}{\partial \tau} + \frac{Aq}{c \rho_0} \\ \frac{\partial W(r, \tau)}{\partial \tau} = a_m \left( \frac{d^2 W(r, \tau)}{dr^2} + \frac{2}{r} \frac{dW(r, \tau)}{dr} \right) + a_m^T \left( \frac{d^2 T(r, \tau)}{dr^2} + \frac{2}{r} \frac{dT(r, \tau)}{dr} \right) \end{cases} \quad (9)$$

With initial conditions

$$T(0, r) = T_n = \text{const} \quad W(0, r) = W_n = \text{const}$$

All mass and heat transfer coefficients ( $a_m, \delta, \lambda$ ) as well as thermodynamic characteristics  $c, r, \varepsilon$  depended on moisture content and temperature. Boundary conditions of the third order, reflecting heat exchange, were:

$$-\lambda \left( \frac{\partial T}{\partial r} \right)_{r=R} + \alpha (T_c - T_n(\tau)) - r_c (1 - \varepsilon) \beta \rho_0 (W_n(\tau) - W_p) + A = 0 \quad (10)$$

where  $A$  is absorbed radiation flow density.

Mass exchange between the body surface and the environment:

$$-\lambda \left( \frac{\partial W}{\partial r} \right)_{r=R} + a_m \delta \left( \frac{\partial T}{\partial r} \right)_{r=R} + \beta (W_n(\tau) - W_p) = 0 \quad (11)$$

Symmetry conditions:

$$\left. \frac{\partial T}{\partial r} \right|_{r=0} = 0 \quad \left. \frac{\partial W}{\partial r} \right|_{r=0} = 0$$

The task was completed under the condition that the boundary was movable and its movement was described by a function  $R(\tau)$ :

$$0 \leq r \leq R(\tau), [R(0) = R_0], \tau > 0$$

The task was the problem of heat and mass conduction with a moving boundary. Due to the dependence of the characteristic size of the area of heat and mass transfer on time, classical methods of separation of variables and integral Fourier transforms were generally not applied to this type of problem, because within the framework of mathematical physics, it was not possible to reconcile the solutions of heat and mass conduction equations with a moving boundary. One of the methods that can be applied to this class of problems was the method of functional transformations or, as it is called, the method of translating a boundary value problem of a generalized type into a classical task.

The resulting system of equations was a mathematical model of the process of drying high-moisture materials. Based on the fact that the heat and mass transfer coefficients, as well as the thermodynamic characteristics, were assumed to be constant, the possible options for applying the model were:

1. Solution of the system of equations of the drying process in a moving coordinate system. In this case, the system of equations was transformed into a moving system of coordinates, and then transformed into a classical system of differential equations, which can be solved by classical methods (separation of variables and integral Fourier transformations, etc.).
2. Zonal method of calculating moisture content and temperature fields. In this case, non-stationary heat and mass exchange was divided into zones. For each zone, the coefficients can be considered constant.

To carry out a zonal calculation, in general case, a zone was understood as a certain time interval  $\Delta\tau_j = \tau_j - \tau_{j-1}$  ( $\tau_{j-1} < \tau_j$ ,  $j = \overline{0, k}$ ,  $\tau_0 = 0$ ,  $\tau_k$  - drying time), during which the heat and mass exchange process took place. At the same time, the following was accepted for each zone:

- The process was described by differential equations in time derivatives;
- The geometric shape of the dried product was constant;
- Thermophysical and mass exchange parameters were averaged;
- The initial distribution of temperature and moisture content by volume of the dried product was constant;
- Heat and mass flow density were constant;
- Division into zones allowed to achieve the necessary accuracy of calculating the temperature and moisture of the product.

3. Application of effective heat and mass transfer coefficients ( $a_{nef}, \delta_{ef}, \lambda_{ef}$ ). In the presence of molar vapour transfer during drying of capillary-porous and colloidal materials containing macropores (at the temperature of the material above 100°C), the influence of concentration and temperature components of molar vapour transfer was taken into account.

The calculation can also be carried out based on the averaged characteristics, which are sometimes called “effective”. However, such a way can be applied only in rare cases, since the issue of parameter averaging usually turns out to be extremely difficult.

Based on the boundary conditions, as well as introducing dimensionless quantities: temperature –  $T$ , moisture –  $W$ , coordinate –  $X = \frac{r}{R}$ , time –  $Fo = \frac{\alpha \cdot \tau}{R^2}$  the following equation and boundary conditions for temperature change were obtained:

$$\frac{\partial T(X, Fo)}{\partial Fo} = \frac{d^2 T(X, Fo)}{dX^2} + \frac{2}{X} \frac{dT(X, Fo)}{dX} - \varepsilon Ko \frac{\partial W(X, Fo)}{\partial Fo} \quad (12)$$

$$\frac{\partial W(X, Fo)}{\partial Fo} = Lu \left( \frac{d^2 W(X, Fo)}{dX^2} + \frac{2}{X} \frac{dW(X, Fo)}{dX} \right) - Lu Pn \left( \frac{d^2 T(X, Fo)}{dX^2} + \frac{2}{X} \frac{dT(X, Fo)}{dX} \right) \quad (13)$$

The tasks were considered to be symmetric:

$$\frac{\partial T(0, Fo)}{\partial X} = \frac{\partial T(0, Fo)}{\partial X} = 0 \quad \begin{cases} T(0, Fo) \neq \infty \\ U(0, Fo) \neq \infty \end{cases}$$

Boundary conditions were:

$$\frac{\partial T(1, Fo)}{\partial X} - Bi_q [1 - T(1, Fo)] + (1 - \varepsilon) Ko \cdot Lu \cdot Ki_m = 0 \quad (14)$$

$$-\frac{\partial U(1, Fo)}{\partial X} + Pn \frac{\partial T(1, Fo)}{\partial X} + Ki_m (Fo) = 0 \quad (15)$$

where  $Fo = \frac{\alpha \tau}{R^2}$  - Fourier criterion (homochromicity number of transfer potential fields);

$Ko = \frac{r \Delta W}{c_m \Delta T}$  - the Kosovych criterion (dependence between the amount of heat spent on the

evaporation of a liquid and on the heating of a wet sample;  $Pn = \frac{\delta \Delta T}{\Delta W}$  Posnov criterion for

diffusion transfer (equal to the ratio of the intensity of thermal diffusion transfer of moisture to diffusion transfer of moisture);  $Lu = \frac{a_m}{a}$  - the Lykov criterion (equal to the ratio of

moisture mass diffusion coefficients to heat diffusion coefficients);  $Bi_q = \frac{aR}{\lambda}$ ,  $Bi_m = \frac{a_m R}{a_m}$  -

heat exchange and mass exchange criterion of Bio;  $Ki = \frac{qR}{\lambda T_c}$  - Kirpichev criterion,

(Sorochinsky, 2019).

### Calculation of the parameters of the thermoradiative-convective drying process

When calculating the criteria the values  $\Delta T = T_c - T_n$ ;  $\Delta W = W_n - W_p$  were taken, where  $T_c, T_n$  the temperature of the environment and the initial temperature of the product;  $W_n, W_p$  - the initial and equilibrium moisture content of the product.

The obtained data are shown in Table 1.

**Table 1**

**Process parameters**

Parameter	Symbol	Unit	Value for			
			Mushrooms	Hawthorn	Apples	Apple snacks
Initial moisture content	$W_n$	%	810	330	715	520
Final moisture content	$W_k$	%	32	38	35	40
Equilibrium moisture content	$W_p$	kg/kg	0.0	0.0	0.0	0.0
The initial temperature of the product	$T_n$	K	297	297	297	297
Coolant temperature	$T_c$	K	333	333	333	333
Particle density	$\rho$	kg/m <sup>3</sup>	750	1173.4	880	965
Specific heat capacity of dry material	$c$	kJ/kg×K	1.420	1.59	3.801	3.768
Thermal conductivity	$\lambda$	W/m×K	0.028	0.112	0.49	0.49
Thermal conductivity coefficient	$a$	m <sup>2</sup> /s	$76 \times 10^{-7}$	$6.3 \times 10^{-6}$	$14.6 \times 10^{-8}$	$13.3 \times 10^{-8}$
Moisture diffusion coefficient	$a_m$	m <sup>2</sup> /s	$9.58 \times 10^{-7}$	$6.8 \times 10^{-7}$	$8,48 \times 10^{-5}$	$8,28 \times 10^{-6}$
Thermal diffusion coefficient	$\delta$	1/K	$1.011 \times 10^{-3}$	$0.51 \times 10^{-2}$	$3,096 \times 10^{-5}$	$4,,06 \times 10^{-2}$
Phase transformation coefficient	$\varepsilon$		0.5	0.5	0.5	0.5
Heat transfer coefficient	$\alpha$	W/m <sup>2</sup> ×K	14	10.417	617.28	396.253
Moisture transfer coefficient	$\beta$	m/s	0.165	0.107	0.086	0.501
Specific heat of vaporization	$r$	kJ/kg	2443	2356.9	2356.9	2356.9

The moisture diffusivity is the highest among the studied products for cultivated mushrooms and is  $9.58 \times 10^{-4}$  m<sup>2</sup>/s, due to the lowest density of 750 kg/m<sup>3</sup> and the highest porosity of the mushroom, which leads to deeper penetration of infrared radiation with a thermal diffusion coefficient of  $1.011 \times 10^{-3}$  1/K. The moisture diffusion coefficient for hawthorn is  $6.8 \times 10^{-7}$  m<sup>2</sup>/s, with a density of 1173.4 kg/m<sup>3</sup> and a thermal diffusion coefficient of  $0.51 \times 10^{-2}$  1/K, due to the fact that the hawthorn fruits are spherical and were placed in the

dryer in a heap. Apples and apple snacks when placed in the dryer were cut into slices of 4–6 mm, for which the moisture diffusion coefficient for apples is  $8.48 \times 10^{-5}$  m<sup>2</sup>/s, with the density of apples 880 kg/m<sup>3</sup> and the thermal diffusion coefficient  $3.096 \times 10^{-5}$  1/K. Apple snacks were made by blanching apple cores in sugar syrup before drying, which led to a decrease in the moisture diffusion coefficient to  $8.28 \times 10^{-6}$  m<sup>2</sup>/s, an increase in density to 965 kg/m<sup>3</sup>, and a thermal diffusion coefficient of  $4.06 \times 10^{-2}$  1/K compared to apple slices.

The solution of the task was obtained in the following form:

$$T(X, Fo) = 1 - \sum_{n=1}^{\infty} \sum_{i=1}^2 c_{ni} \Phi_{\Gamma}(v_i \mu_n X) \exp(-\mu_n^2 Fo) \quad (16)$$

$$U(X, Fo) = 1 + \frac{1}{\varepsilon Ko} \sum_{n=1}^{\infty} \sum_{i=1}^2 c_{ni} (1 - v_i^2) \Phi_{\Gamma}(v_i \mu_n X) \exp(-\mu_n^2 Fo) \quad (17)$$

where

$$v_i^2 = \frac{1}{2} \left[ \left( 1 + KoPn + \frac{1}{Lu} \right) + (-1)^i \sqrt{\left( 1 + KoPn + \frac{1}{Lu} \right)^2 - \frac{4}{Lu}} \right] \quad (18)$$

$$v_1^2 = \frac{1}{2} \left( 80.366 - \sqrt{80.366^2 - \frac{4}{Lu}} \right) = 1 \left( 80.366 + \sqrt{80.366^2 - \frac{4}{Lu}} \right) = 8.909$$

$$c_{n1} = \frac{2}{\mu_n \Psi_n} \left| (1 - \varepsilon KoK1) P_{n2} + \varepsilon KoQ_{n2} \right| \quad c_{n2} = -\frac{2}{\mu_n \Psi_n} \left| (1 - \varepsilon KoK1) P_{n1} + \varepsilon KoQ_{n1} \right| \quad (19)$$

$$\Psi_n = v_1 A_{n1} P_{n2} + v_2 B_{n2} Q_{n1} - v_2 A_{n2} P_{n1} - v_1 B_{n2} Q_{n2} \quad (20)$$

The separation of variables by the Fourier method allowed to advance much further than in the general case.

$$Q_{n1} = \left( 1 - \frac{1}{Bi_q} + (1 - v_1^2) K1 \right) \sin(v_i \mu_n) + \frac{1}{Bi_q} v_i \mu_n \cos(v_i \mu_n) \quad (21)$$

$$P_{ni} = (1 - v_i^2) \sin(v_i \mu_n) + \frac{(1 - v_i^2) + \varepsilon KoPn}{Bi_m} (v_i \mu_n \cos(v_i \mu_n) - \sin(v_i \mu_n)) \quad (22)$$

$$A_{ni} = \left[ 1 + (1 - v_i^2) K1 \right] \cos(v_i \mu_n) - \frac{1}{Bi_q} v_i \mu_n \sin(v_i \mu_n) \quad (23)$$

$$B_{ni} = (1 - v_i^2) \cos(v_i \mu_n) - \frac{(1 - v_i^2) + \varepsilon KoPn}{Bi_m} v_i \mu_n \sin(v_i \mu_n) \quad (24)$$

where  $\mu_n$  is roots of the characteristic equation

$$P_{n1} Q_{n2} - P_{n2} Q_{n1} = 0 \quad (25)$$

$$K1 - \text{value: } K1 = \frac{1 - \varepsilon}{\varepsilon} Lu \frac{Ki_m}{Bi_q} \quad (26)$$

The averaged heat and mass transfer potentials were calculated according to the following dependencies:

$$\bar{T}(Fo) = 1 + \sum_{n=1}^{\infty} \sum_{i=1}^2 D_{ni} \exp(-\mu_n^2 Fo) \quad (27)$$

$$\bar{U}(Fo) = 1 - \frac{1}{\varepsilon Ko} \sum_{n=1}^{\infty} \sum_{i=1}^2 D_{ni} (1 - v_i^2) \exp(-\mu_n^2 Fo) \quad (28)$$

$$D_{ni} = 3C_{ni} \frac{\sin(v_i \mu_n) - v_i \mu_n \cos(v_i \mu_n)}{(v_i \mu_n)^2} \quad (29)$$

The obtained system of differential transport equations together with the initial and boundary conditions reflects in an analytical form the main features of the studied process of thermoradiative-convective drying of high-moisture materials, that is, it is its mathematical model. The solution of the model makes it possible to obtain a complete picture of the distribution of transfer potentials in a body or a system of bodies, to trace the change of potential fields over time, and on this basis to provide a detailed analysis of the kinetics and dynamics of the process of drying high-moisture materials.

### Comparative analysis of analytical and calculation data of thermoradiative-convective drying

A software module for calculating the drying process of high-moisture materials during thermoradiative-convective dehydration has been developed. The result of the approximation of experimental data regarding the drying of particles of cultivated mushrooms, hawthorn, apples, and apple snacks is shown in Figure 3. Comparative analysis of calculated and experimental data showed good convergence: the deviation of calculated data from experimental data did not exceed 9.6%.

The obtained data are shown in Table 2.

When processing the data of Figure 4, for the dehydration of cultivated mushrooms, which is traced by a decrease in moisture content from 809 to 30%, it is necessary to spend 80 minutes, and to reduce the moisture content of hawthorn from 330 to 38%, the duration of the thermoradiative-convective drying process is 60 minutes.

The duration of drying of apple snacks increases by 10 minutes compared to apples, which is due to the sugar content in the snacks and the osmotic properties of sugar to retain moisture, which is characterized by the viscosity of colloids (Strelchenko et al., 2019). When drying, it is necessary to give the snacks more heat to loosen the colloid bonds and remove moisture from the product.

Comparative analysis of calculated and experimental data shows a satisfactory convergence: the deviation of calculated data from experimental data did not exceed 9.6% during thermoradiative-convective drying and is due to the fact that the model does not take into account all factors that affect the process, as well as simplifications, allowed in the model itself.

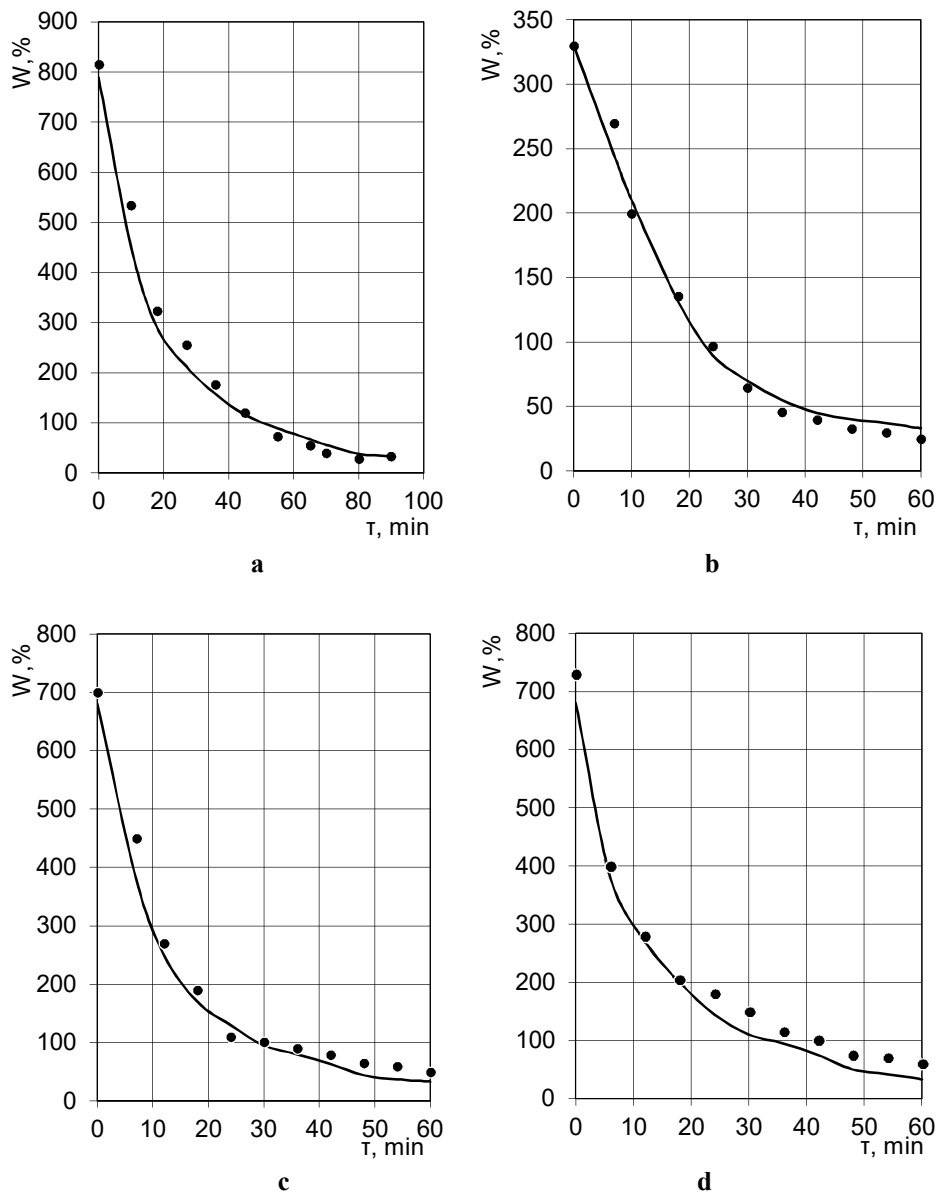


**Figure 3. Change in moisture content of high-moisture materials over time**

$W$  is moisture content, %;  $\tau$  is drying time, min.

a is cultivated mushrooms; b is hawthorn; c is apples; d is apple snacks.

● – experimental data

— – calculated data



**Table 2**  
**Comparative analysis of experimental and calculated data of thermoradiative-convective drying**  
**of products of plant origin**

Duration, min	W <sub>m</sub> (model), %		W <sub>e</sub> (experimental), %		Relative difference, %	
	Cultivated mushrooms	Hawthorn	Cultivated mushrooms	Hawthorn	Cultivated mushrooms	Hawthorn
0	789	324	809	330	7.991	1.8
9	450	238	534	247	4.753	9.0
18	296	177	312	174	5.1	1.7
27	212	132	233	134	9.0	1.5
36	157	98.5	177	95	1.671	0.96
45	118	71.4	116	66	1.169	7.6
54	89	52.7	81	48	8.9	8.9
63	77	40.7	71	38	7.8	6.6
81	38	-	35	-	7.9	-
90	33	-	32	-	3.0	-
Duration, min	Apples	Apple snacks	Apples	Apple snacks	Apples	Apple snacks
0	680	487	713	517	7.056	5.8
7	380	360	450	380	4.733	5.2
12	251	270	270	279	3.116	3.3
18	170	200	190	205	2.206	2.4
24	130	145	110	158	1.493	8.2
30	95	120	102	130	1.185	7.7
36	80	92	87	100	0.917	8.0
42	64	75	82	83	0.731	9.6
48	44	55	65	64	0.593	9.0
54	37	42	60	50	0.508	8.0
60	33	40	50	48	0.366	8.0

## Conclusions

1. The developed energy-efficient chamber thermoradiative-convective dryer with the combined interaction of infrared radiation and an additionally installed heat pump will make it possible to reduce energy costs for the drying process by up to 30%. The developed design of the technological channels of the dryer due to the additional supply and removal of air in the side walls of the dryer allows avoiding stagnant zones and uniform distribution of air.
2. For the first time, a comparison of the kinetics of thermoradiative-convective drying of the drying process of cultivated mushrooms, hawthorn, apples, and apple snacks was investigated, which showed a decrease in duration compared to convective drying and an improvement in the quality of products compared to thermoradiative drying.
3. Calculated moisture diffusion coefficients of thermoradiative-convective drying in the middle of products, which are for cultivated mushrooms –  $9,58 \times 10^{-4}$  m<sup>2</sup>/s, hawthorn –  $6.8 \times 10^{-7}$  m<sup>2</sup>/s, apples –  $8.48 \times 10^{-5}$  m<sup>2</sup>/s and apple snacks –  $8.28 \times 10^{-6}$  m<sup>2</sup>/s.

4. A system of differential transport equations was obtained, which allows to display in an analytical form the main features of the simultaneous influence of convective and thermoradiative energy supply during drying of high-moisture materials with a discrepancy between experimental and calculated data of up to 9.6%.

## References

- Akter F., Muhury R., Sultana A., Kumar Deb U. (2022), Comprehensive review of mathematical modeling for drying processes of fruits and vegetables, *International Journal of Food Science*, 8, pp. 1–10, <https://doi.org/10.1155/2022/6195257>
- Argyropoulos D., Heindl A., Müller J. (2011), Assessment of convection, hot-air combined with microwave-vacuum and freeze-drying methods for mushrooms with regard to product quality, *International Journal of Food Science & Technology*, 46(2), pp. 333–342, <https://doi.org/10.1111/j.1365-2621.2010.02500.x>
- Arumuganathan T., Manikantan M.R., Rai R.D., Anandakumar S., Khare, V. (2009), Mathematical modelling of drying kinetics of milky mushroom in a fluidized bed dryer, *International Agrophys*, 23(1), pp. 1–7.
- Bhattacharya M., Srivastav P., Mishra H. (2013), Thin-layer modelling of convective and microwave-convective drying of oyster mushroom (*Pleurotus ostreatus*), *Journal of Food Science and Technology*, 52(4), pp. 2013–2022, <https://doi.org/10.1007/s13197-013-1209-2>
- Bennamoun L., Khama R., Léonard A. (2015), Convective drying of single cherry tomato: modeling and experimental study, *Food and Bioproducts Processing*, 94, pp. 114–123, <https://doi.org/10.1016/j.fbp.2015.02.006>
- Coşkun S., Doymaz's İ. (2017), Investigation of drying kinetics of tomato slices dried by using a closed loop heat pump dryer, *Heat and Mass Transfer*, 53(6), pp. 1–9, <https://doi.org/10.1007/s00231-016-1946-7>
- Giri S., Prasad S. (2007), Drying kinetics and rehydration characteristics of microwave-vacuum and convective hot-air dried mushrooms, *Journal of Food Engineering*, 78, pp. 512–521, <https://doi.org/10.1016/j.jfoodeng.2005.10.021>
- Gunhan T., Demir V., Hancioglu E., Hepbasli A. (2005), Mathematical modelling of drying of bay leaves, *Energy Conversion and Management*, 46(11–12), pp. 1667–1679, <https://doi.org/10.1016/j.enconman.2004.10.001>
- Dubkovetskiy I., Yurchak V., Rak V., Burlaka T., Kazmiryshen V. (2019), Research of methods and modes of drying of gluten-free pasta, *Journal of Hygienic Engineering and Design*, 29, pp. 151–159.
- Hayvas B. (2010), Mathematical modelling of materials convective drying with allowance for coupled mechanical, thermal and diffusive processes, *Physico-Mathematical Modeling and Information Technologies*, 2, pp. 9–37.
- Maisnam D., Rasane P., Dey A., Kaur S., Sarma C. (2017), Recent advances in conventional drying of foods, *Journal of Food Technology and Preservation*, 1(1), pp. 25–34.
- Menges H., Ertekin C. (2006), Mathematical modeling of thin layer drying of Golden apples, *Journal of Food Engineering*, 77, pp. 119–125, <https://doi.org/10.1016/j.jfoodeng.2005.06.049>
- Pal U., Chakraverty A. (1997), Thin layer convection-drying of mushrooms, *Energy Conversion and Management*, 38, pp. 107–113, <https://doi.org/10.1111/j.1745-4549.2008.00300.x>

- Petrova Z., Slobodianiuk K. (2017), Energy effective drying modes of soy-vegetable compositions, *Ukrainian Journal of Food Science*, 5(1), pp. 122–132, <https://doi.org/10.24263/2310-1008-2017-5-1-15>
- Sabarez H. (2015), Modelling of drying processes for food materials, In: S. Bakalis, K. Knoerzer, P.J. Fryer (Eds.), *Modelling Food Processing Operations*, Elsevier, pp. 95–127, <https://doi.org/10.1016/B978-1-78242-284-6.00004-0>
- Sharma G., Verma R., Pathare P. (2005), Mathematical modeling of infrared radiation thin layer drying of onion slices, *Journal of Food Engineering*, 71(3), 282, <https://doi.org/10.1016/j.jfoodeng.2005.02.010>
- Sorochinsky V. (2019), The influence of convective drying on the change of Kirpichev mass-exchange criterion, *Journal of Physics: Conference Series*, 1399(2), 022012, <https://doi.org/10.1088/1742-6596/1399/2/022012>
- Sorokova N., Didur V., Variny M. (2022), Mathematical modeling of heat and mass transfer during moisture–heat treatment of castor beans to improve the quality of vegetable oil, *Agriculture*, 12, 1356, <https://doi.org/10.3390/agriculture12091356>
- Strelchenko L., Dubkovetskyi I., Malejik I. (2019), Influence of differential heat treatment on foodstuffs with apples obtained by the convection-thermoradiation method of drying, *Ukrainian Food Journal*, 8(1), pp. 155–169, <https://doi.org/10.24263/2304-974X-2019-8-1-15>
- Wang J., Sheng K. (2006), Far-infrared and microwave drying of peach, *LWT – Food Science and Technology*, 39(3), pp. 247–255, <https://doi.org/10.1016/j.lwt.2005.02.001>
- Zecchi B., Clavijo L., Martínez Garreiro J., Gerla P. (2011), Modeling and minimizing process time of combined convective and vacuum drying of mushrooms and parsley, *Journal of Food Engineering*, 104, pp. 49–55, <https://doi.org/10.1016/j.jfoodeng.2010.11.026>